Structural Biology of Human Metal-Dependent Histone Deacetylases

Matthieu Schapira

Structural Genomics Consortium, and Department of Pharmacology & Toxicology, University of Toronto, 101 College st, Toronto, ON, Canada

Abstract

Class I, II and IV histone deacetylases (HDACs) are metal-dependent enzymes involved in a broad and partly unexplored array of biological mechanisms that include epigenetic control of gene expression. The catalytic domain of human class I and IIa enzymes has been solved in complex with a substrate peptide and inhibitors, which revealed a conserved architecture, uncovered the catalytic mechanism of deacetylation, and outlined a chemical framework for inhibitor design. We will review the different structural elements of metal-dependent HDACs and their contribution to substrate recognition, catalysis, and inhibitor specificity.

Introduction

Histone deacetylases (HDACs) are important regulators of cellular mechanisms, generally operating within large multiprotein complexes, and remove acetyl marks from lysine side-chains of target proteins. Deacetylation of histone proteins by HDACs mediates the epigenetic control of gene expression and cellular differentiation (Grozinger and Schreiber 2002). Additionally, it is now clear that the regulatory role of protein acetylation extends vastly beyond epigenetic mechanisms (Choudhary et al. 2009) and so is the expected scope of HDAC biology. Some HDAC inhibitors are approved anti-cancer agents, and applications in other therapeutic areas are investigated, as more compounds with diverse selectivity profiles are being developed (Bradner et al. ; Marks ; Xu et al. 2007).

Human HDACs are divided into five evolutionarily related classes based on phylogenetic analysis (Gregoretti et al. 2004) (Figure 1): HDAC1,2,3,8 (class I), HDAC4,5,7,9 (class IIa), HDAC6,10 (Class IIb), the sirtuins SIRT1-7 (Class III), and HDAC11 (Class IV). Classe I, II, and IV enzymes require a divalent metal ion for catalysis. Sirtuins are NAD+-dependent enzymes structurally and biochemically unrelated to other classes, and will not be discussed in this review (Sauve et al. 2006). The first structure of an HDAC catalytic domain was that of a bacterial protein sharing 35% sequence identity with human HDAC1, and revealed a topology similar to arginase (Finnin et al. 1999; Kanyo et al. 1996). Structures of human HDAC2 (Bressi et al.), HDAC4 (Bottomley et al. 2008), HDAC7 (Schuetz et al. 2008) and HDAC8 (Dowling et al. 2008; Dowling et al. ; Somoza et al. 2004; Vannini et al. 2004; Vannini et al. 2007) solved since confirmed the general architecture revealed by the seminal work on the bacterial enzyme, and define a set of canonical features (Figure 2): (1) a funnel-shaped lysine binding channel located at the center of an overall α/β fold, (2) a combination of conserved catalytic residues organized around the catalytic Zn ion at the bottom of the channel and (3) a set of loops with variable length and flexibility at the rim of the channel, forming protein interaction

interfaces. These features play different roles in substrate recognition, catalytic mechanism and inhibitors specificity, which will be reviewed in the following sections.

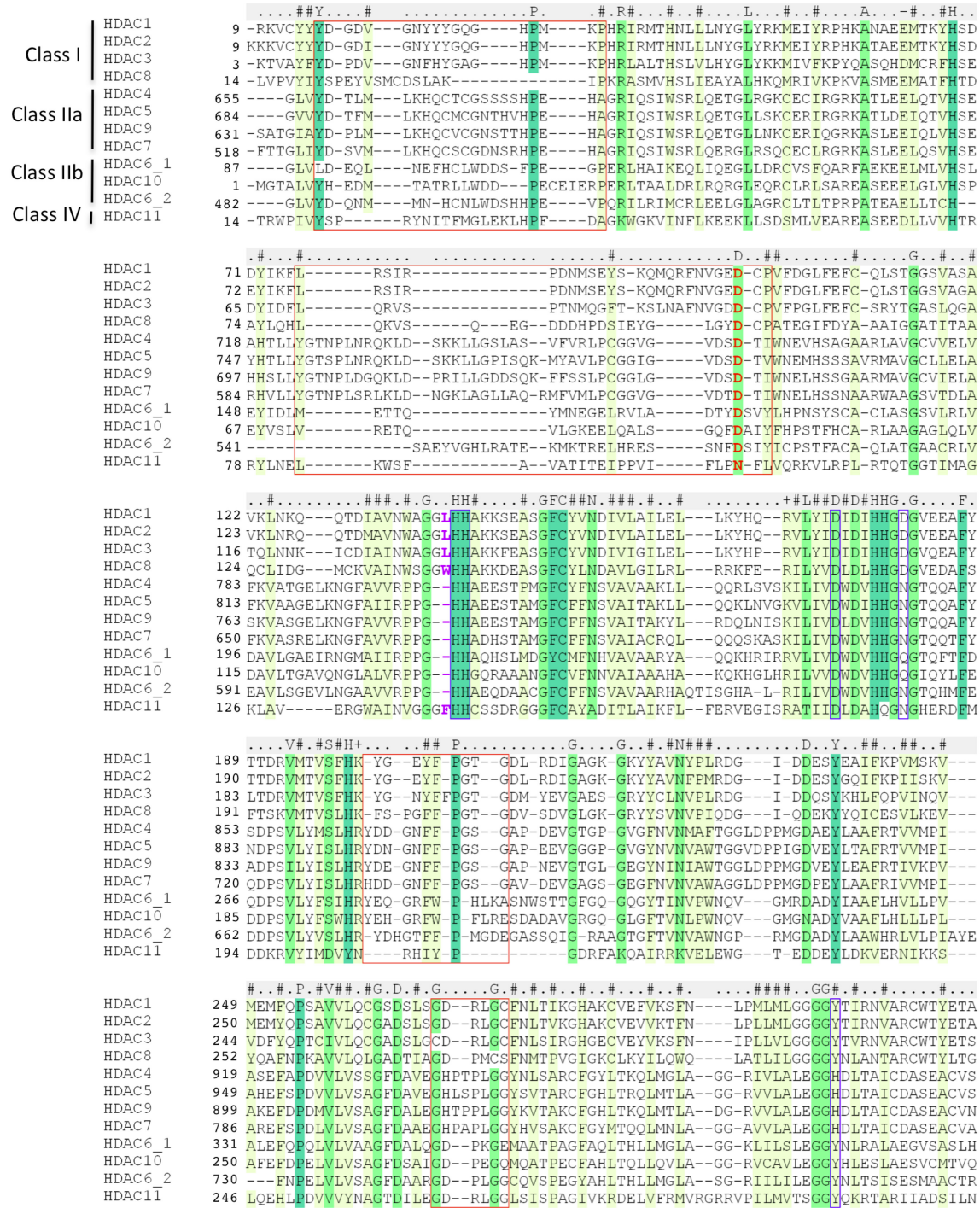

Figure 1: Sequence alignment of the catalytic domain of human metal-dependent HDACs. Variable loops L1 to L4 are delimited by red boxes. Catalytic residues: blue boxes. The conserved aspartate at the rim is highlighted in red. The residue opening or closing the foot pocket in class I enzymes is in magenta. The alignment was generated with ICM (Molsoft LLC) from a seed alignment of 157 sequences downloaded from the PFAM database (domain PF00850). Variable regions were manually edited based on available structures. Both catalytic domains of HDAC6 are shown.

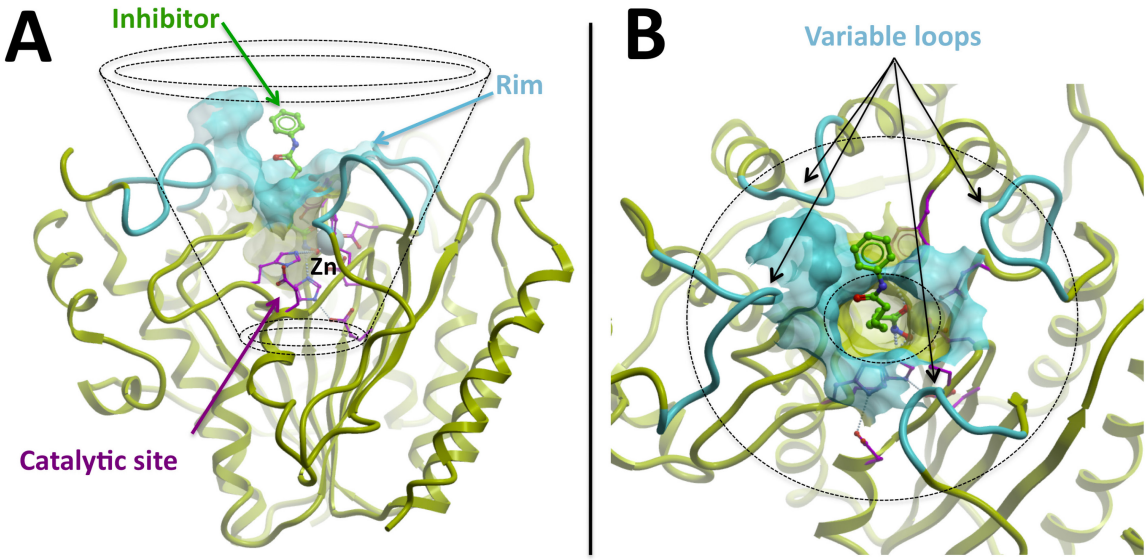

Figure 2: Overall structure of HDAC catalytic domains. Side (A) and top (B) views of HDAC8 in complex with the inhibitor SAHA [pdb code: 1t69] (Somoza et al. 2004) show that the catalytic domain is composed of (1) a structurally conserved core (mustard), (2) a rim made of variable loops (cyan) where substrate recognition is expected to occur and (3) a lysine binding channel leading to the catalytic site (magenta), organized around a zinc ion (gray ball). All co-crystallized inhibitors to date occupy the central channel of HDACs and participate in the coordination of the zinc, as illustrated here by the bound conformation of SAHA (green). Oxygen and nitrogen atoms are colored red and blue respectively.

Substrate Recognition

Insertion of the acetylated lysine side-chain into the central channel of HDACs implies that the rim of the channel is in direct contact with protein substrates. This rim is mainly composed of a set of four loops (named L1-L4) with variable sizes and conformations between different HDAC isoforms, and between different structures of a same isoform for L1 and L2 (Figure 3A-E). Importantly, these loops are often

found at the interface of crystallographic dimers in HDAC structures, which probably reflects their propensity to act as protein interaction interface.

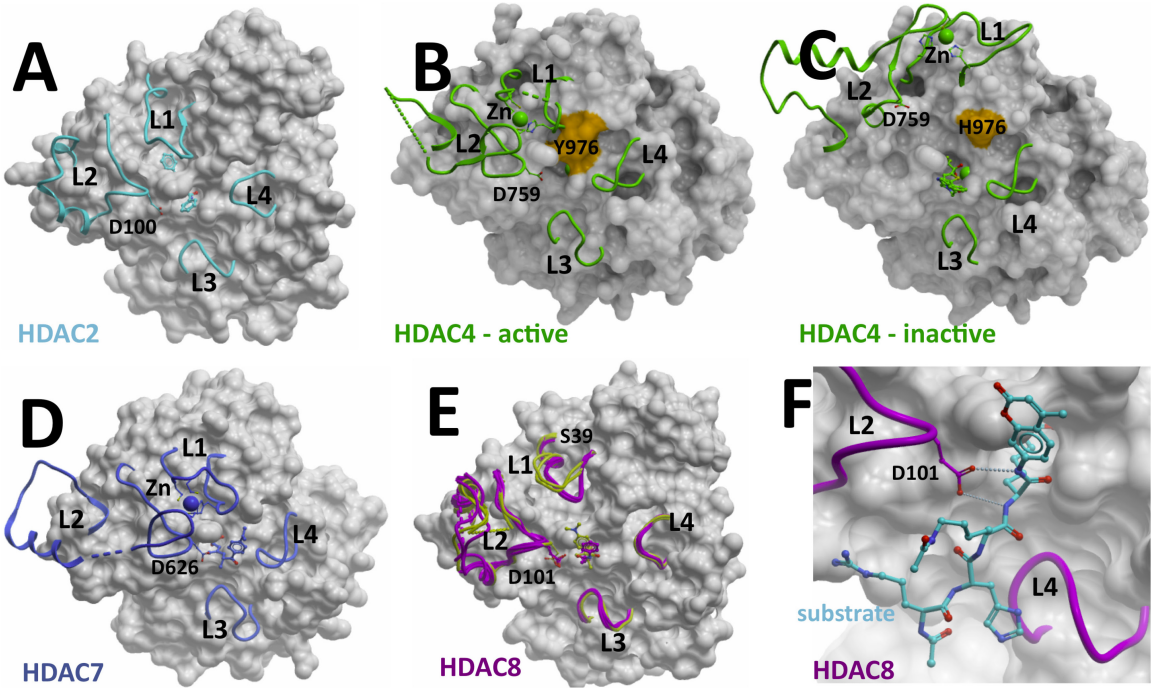

Figure 3: Variability and flexibility of loops forming the rim. While the core structure of the catalytic domain is well conserved (symbolized here by a white molecular surface representation where loops have been truncated – orientation as in Figure 1B), the length and conformation of the loops at the rim of the lysine-binding channel are extremely variable, which probably contributes to substrate specificity. A: HDAC2 bound to an N-(2-amino phenyl) benzamide inhibitor ([pdb code: 3max], (Bressi et al.)). B: inhibitor-free, gain-of-function HDAC4 mutant (H976Y – orange) ([2vqw], (Bottomley et al. 2008)). C: HDAC4 bound to a trifluoromethyl-ketone inhibitor ([2vqj], (Bottomley et al. 2008)). D: HDAC7 bound to TSA ([3c10], (Schuetz et al. 2008)). E: HDAC8. Magenta: loops from HDAC8 bound to a peptide substrate ([2v5w], (Vannini et al. 2007)), and inhibitors MS-344 ([1t67], (Somoza et al. 2004)), SAHA ([1t69], (Somoza et al. 2004)) (shown), and APHA ([3f07], (Dowling et al. 2008)). Yellow: loops from HDAC8 bound to inhibitors TSA ([1t64], (Somoza et al. 2004)) (shown) and CRA-19156 ([1vkg], (Somoza et al. 2004)). F: HDAC8 bound to a tetrapeptide substrate (cyan) ([2v5w], (Vannini et al. 2007)).

A structure of HDAC8 in complex with an acetylated tetrapeptide shows that residues from L2 and L4 are in direct contact with the acetylated lysine. Asp101 of loop L2 makes two hydrogen-bonds with the backbone nitrogen atoms flanking the

substrate lysine, and constrains the peptide in a cis-conformation (Vannini et al. 2007) (Figure 3F). Asp 101 is the only residue from the L2 loop that is absolutely conserved across all HDACs (except for HDAC11) (Figure 1), and is positioned at the entrance of the lysine channel in structures of all human HDACs solved to date (Figure 3A,B,D,E). D101 mutations result in loss of HDAC8 activity on peptide and purified histone substrates (Dowling et al. 2008; Vannini et al. 2007); HDAC4 activity is similarly antagonized by mutation of the corresponding D759 to Ala (Bottomley et al. 2008). These observations suggest that the interaction between D101 and substrates is critical in positioning HDAC8 substrates, and that this mechanism is conserved in other HDACs.

Class IIa HDACs are characterized by short and large inserts in their L1 and L2 loops respectively. Two Cys and one His from L1 and one Cys from L2 coordinate a Zn ion in these enzymes, which is believed to stabilize the large and flexible loops. These Zn coordinating cystein residues can be oxidized and reduced in cells, which affects nuclear localization of HDAC4, and may be linked to cardiac hypertrophy in vivo (Ago et al. 2008). Their mutation abrogates interaction with the co-repressor complex N-CoR-HDAC3 (Bottomley et al. 2008). The structural Zn places Asp626 of HDAC7 (the equivalent Asp101 in HDAC8) at the entrance of the lysine channel, in its putative catalytically competent conformation (Figure 3D). The same conformation is observed in the apo structure of the gain-of-function H976Y HDAC4 mutant (Figure 3B). Surprisingly, in the structure of wild type HDAC4 in complex with a trifluoromethylketone inhibitor, L1 and L2 loops adopt very different conformations, the structural Zn is coordinated by a different set of residues, and the conserved L2 aspartate (D759) is positioned far from the lysine channel (Figure 3C). Superimposition of the two HDAC4 structures shows that the inhibitor occupying the lysine channel in the wild type structure clashes with the conformation of the conserved L2 D759 observed in the active structure. It is unclear whether small structural adjustments would be sufficient to resolve this clash, but this observation reveals a possible allosteric mechanism of inhibition

whereby inhibitors would not necessarily occupy the catalytic site, but would prevent positioning of the L2 aspartate at the entrance of the lysine channel.

Structural variations are also observed between different structures of class I enzymes. For instance, different HDAC8 structures reveal alternate conformations of the L1 and L2 loops. L1 seems to adopt one of two possible conformations, while L2, larger and more flexible, is not always structured (Figure 3E). Ser39 is a phosphorylation site in HDAC8 only 5A away from Lys36 of the L1 loop; this post-translational modification is accompanied by decreased activity, which could be mediated by the destabilization of an active L1 conformation (Lee et al. 2004; Somoza et al. 2004).

The diversity in size and conformation of the L1 and L2 loops translates in structurally and electrostatically diverse molecular surfaces (Figure 4), and probably protein interaction interfaces. While the electrostatic potential around the rim is generally electro-negative, which would favor electropositive substrates (such as histone tails) or interaction partners, this property appears much less pronounced in the HDAC2 structure, which may indicate different substrate specificity. In the HDAC8-Trichostatin A (TSA) complex, L1 is more distant from the lysine channel, probably because the dimethylaniline group of TSA would clash with the L1 conformation observed in the substrate-bound structure. This uncovers a secondary pocket, next to, but distinct from the lysine channel, occupied by another TSA molecule in the structure (Figure 4E). This pocket is absent from the substrate-bound conformation (Figure 4F), and may be exploited to design selective inhibitors. Similarly, in the inactive structure of wild type HDAC4, the “open” conformation of L1 and L2 defines a large electropositive cavity (Figure 4C) that is absent from the active conformation (Figure 4B). The two structures capture protein interaction interfaces that vary drastically in shape and electrostatics. This raises the possibility that different binding partners may stabilize the protein in different activation states.

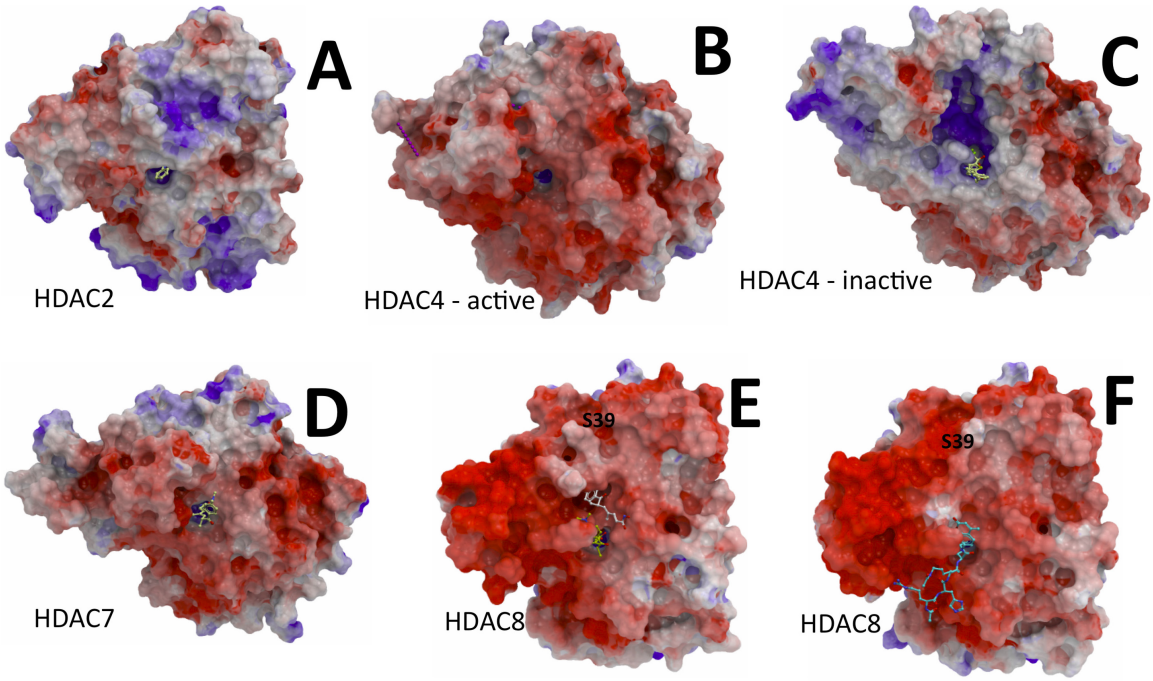

Figure 4: Electrostatics of HDACs. Coloring the molecular surface according to the electrostatic potential (red: electronegative, blue: electropositive) reveals a significant diversity in charge distribution among HDACs that is expected to contribute to substrate specificity. Structure orientations are the same as in Figure 3. Alternate conformations of loops L1 and L2 captured in different structures of HDAC4 (B,C) or HDAC8 (E,F) induce dramatic variations in shape and electrostatics that alter protein interaction interfaces. A large electropositive pocket in HDAC4 (C) and a small cleft occupied by a second TSA molecule (white sticks) in HDAC8 (E) may be exploited to develop inhibitors that would lock the protein in a specific conformation. A: HDAC2 bound to an N-(2-amino phenyl) benzamide inhibitor ([3max], (Bressi et al.)). B: inhibitor-free, gain-of-function HDAC4 mutant (H976Y – orange) ([2vqw], (Bottomley et al. 2008)). C: HDAC4 bound to a trifluoromethyl-ketone inhibitor ([2vqj], (Bottomley et al. 2008)). D: HDAC7 bound to TSA ([3c10], (Schuetz et al. 2008)). E: HDAC8 bound to TSA ([1t64], (Somoza et al. 2004)). F: HDAC8 bound to a tetrapeptide substrate ([2v5w], (Vannini et al. 2007)).

Importantly, a conserved tyrosine residue located at the entrance of the lysine channel is mutated to histidine in Class IIa HDACs (H976 in HDAC4, H843 in HDAC7 – Figure 1). This variation is associated with a 1000-fold loss in catalytic activity, which can be rescued by His to Tyr gain-of-function mutation, as shown in HDAC4, 5 and 7 (Lahm et al. 2007; Schuetz et al. 2008). While a tyrosine side-chain at this position invariably points towards the catalytic site (and participates in catalysis, as discussed later), the histidine side-chain is flipped away from the catalytic site, and

projects towards the solvent. It is tempting to speculate that the conformation of this surface-exposed His at the rim of Class IIa HDACs (Figure 3B,C) is linked to catalytic activity (as discussed later in greater details) and may be controlled by protein interaction events.

In conclusion, most HDACs are found within large multi-protein complexes that regulate substrate specificity and function (Nicolas et al. 2007; Verdin et al. 2003; Yang and Seto 2003). The genetic diversity and the flexibility of loops at the rim of the substrate lysine channel underlie a diverse and malleable molecular surface that can accommodate combinations of substrates and binding partners with diverse shapes and electrostatics. Specific conformational states of the loops captured experimentally revealed non-canonical binding pockets that may be exploited towards allosteric inhibition, but the chemical tractability of these putative binding sites has not yet been validated.

Catalytic Mechanism

The catalytic mechanism of metal-dependent HDACs was originally deduced from the crystal structure of a bacterial HDAC-like protein, and later confirmed by the structure of HDAC8 in complex with a p53 tetrapeptide substrate (Dowling et al. 2008; Finnin et al. 1999; Vannini et al. 2007) (Figure 5A). A catalytic zinc ion polarizes the carbonyl group of the departing acetate, and increases the electrophilicity of its carbonyl carbon. Additionally, the Zn orientates a catalytic water molecule located next to the scissile bond. A pair of conserved histidine residues (H142 and H143 in HDAC8) form hydrogen-bonds with the water molecule and enhance its nucleophilic property. The basicity of H142 is itself increased by a conserved aspartatic acid (D176), completing a charge-relay system. The aspartate is additionally polarized by a neighboring potassium ion. Nucleophilic attack of the substrate's carbonyl carbon by the water molecule is followed by hydrolysis where the hydroxyl group of a neighboring tyrosine (Y306 in HDAC8), initially engaged in a hydrogen-bond with the acetyl carbonyl oxygen, would donate a proton to the amine.

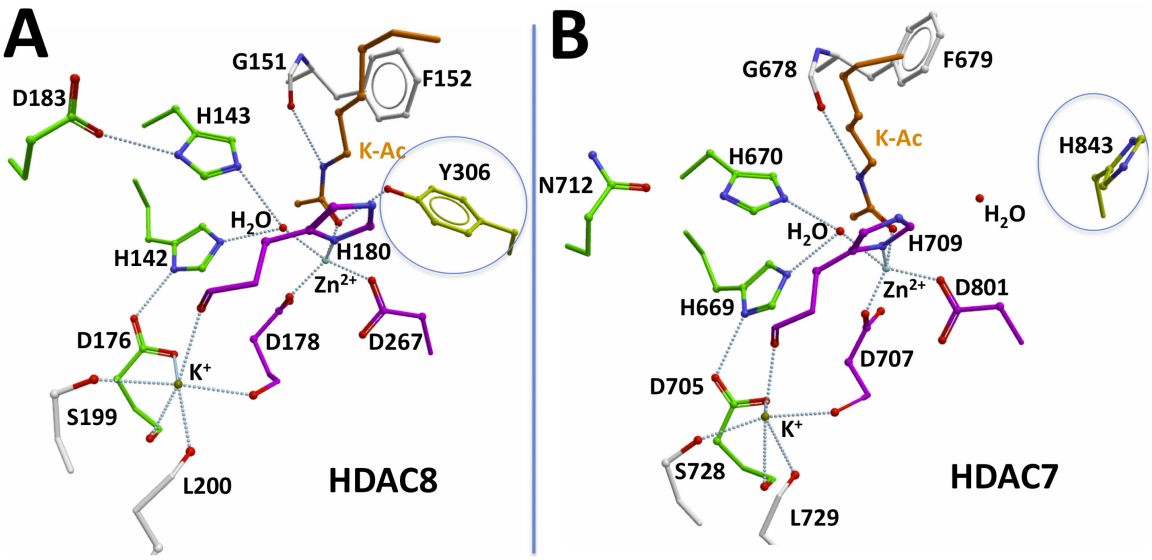

Figure 5: HDAC catalytic mechanism. A- Crystal structure of HDAC8 in complex with an acetylated peptide substrate (orange) ([2v5w] (Vannini et al. 2007), [3ewf] (Dowling et al. 2008)). D176 and D183 polarize H142 and H143 in a charge-relay system (green) that enhances the nucleophilicity of a catalytic water molecule. The latter attacks the carbonyl carbon of the substrate, which is particularly susceptible through its contribution to the coordination system (magenta) of a neighboring zinc ion. The hydroxyl moiety of Y306 forms a hydrogen-bond with the substrate's carbonyl oxygen, and protonates the amino group of the reaction product. (A wild-type tyrosine is shown at position 306, as seen in [3ewf], and a wild type histidine is shown at position 143, as seen in [2v5w], though one or the other residue was mutated in the two structures to capture the complex with a catalytically dead form of the enzyme.). B- The catalytic site of class IIa HDACs, such as apo-HDAC7 shown here ([3c0y] (Schuetz et al. 2008)) with substrate from superimposed HDAC8 [2v5w], differs in one important way (circled): the catalytic tyrosine is replaced by a histidine (H843 in HDAC7). Oxygen: red. Nitrogen: blue.

A water-filled channel linking the active site to the outer molecular surface can be observed in some some HDAC structures, including HDAC8, and was proposed to act as a way of evacuation for the acetate byproduct (Finnin et al. 1999; Nielsen et al. 2005; Vannini et al. 2004) (Figure 6). A conserved arginine is located at the entrance of the tunnel, and may attract the departing acetate through long-range electrostatics. In HDAC8, Ser39 is positioned at the exit of the evacuation channel, and phosphorylation of this residue by PKA inhibits deacetylase activity (Lee et al. 2004), raising the possibility that structural rearrangements induced by the

phosphorylation event affect the release of the reaction by-product, thereby inhibiting turn-over and catalysis. Whether HDAC exit channels are chemically tractable remains an open question.

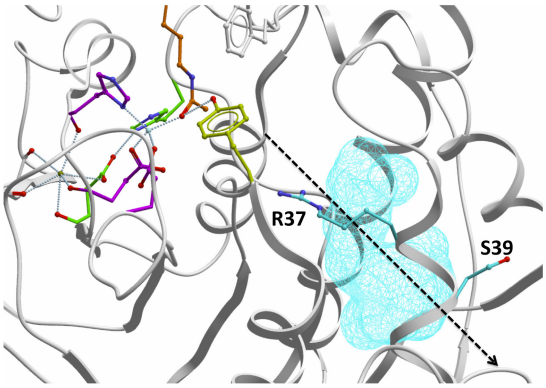

Figure 6: Exit channel. A water-filled channel (cyan) can be observed in some HDAC structures (HDAC8 shown here [2v5w], (Vannini et al. 2007)). The channel links the catalytic site to the outer surface of the protein, and may be used to evacuate the departing acetate. A conserved arginine in the vicinity of the catalytic tyrosine (R37 here) may guide the enzymatic by-product to the entrance of the channel after cleavage of the scissile bond. Phosphorylation events reported at S39 affect the structure at the channel output, and may regulate release of the acetate.

While it is clear that non-class III HDACs are metal-dependent enzymes, the identity of the metal in vivo remains uncertain. HDAC8 activity increases when Zn^{2+} is substituted by Fe^{2+} (Gantt et al. 2006). And, while affinity for Zn^{2+} is about 5 orders of magnitude higher than for Fe^{2+}, cellular levels of Fe^{2+} are 3 to 5 orders of magnitude higher than Zn^{2+} (Dowling et al.). It was also reported that recombinant HDAC8 purified from E. coli contains eight-fold more iron than zinc before dialysis (Gantt et al. 2006). The nature of the metal should nevertheless not affect the catalytic mechanism derived from zinc-bound structures.

Most residues participating in this mechanism are conserved across HDACs, with one important exception: in Class IIa HDACs, the catalytic tyrosine, which is essential for HDAC8 to deacetylate peptidic substrates and purified histones (Vannini et al. 2007) is replaced by a histidine (Y306 in HDAC8, H843 in HDAC7, H976 in HDAC4 - Figures 1 and 5). This does not seem to affect significantly binding of acetylated peptides to HDAC7, but dramatically reduces catalytic activity of Class IIa enzymes (Bottomley et al. 2008; Lahm et al. 2007; Schuetz et al. 2008). Conversely, the H843Y HDAC7 mutant has a similar affinity than wild type for peptide substrates, but is over 5000 times more active (Schuetz et al. 2008).

In HDAC7, H843A and H843F mutants are 60 times less active than H843Y but 80 times more active than the wild type enzyme, indicating that the loss of the tyrosine's hydroxyl group that engages in a hydrogen-bond with the substrate's carbonyl and protonates the reaction product in non-class IIa HDACs accounts only in part for the negative impact of a histidine at this position (Schuetz et al. 2008). This raises the possibility that forcing the histidine side-chain to project towards the catalytic site rather than the protein surface would rescue in part catalytic activity to levels observed in the H843A or H843F mutants. The nitrogen of the scissile bond could possibly accept a proton from a second water molecule observed in the HDAC7 and HDAC4 structures [3c0y, 2vqq] (Figure 5B), or from the second conserved histidine (H670 in HDAC7), as initially proposed for the bacterial HDAC-like protein (Finnin et al. 1999). The latter seems however less likely since the basicity of this second histidine is enhanced by a neighboring aspartic acid present only in Class I enzymes (D183 in HDAC8, N712 in HDAC7 - Figure 1).

It is not clear whether the dramatic loss in enzymatic activity observed biochemically for Class IIa HDACs equally applies *in vivo*. The observation that H843A and H843F HDAC7 mutants are 80 times more active than wild-type suggests that conformational rearrangement of the histidine, possibly induced by protein interaction events, may rescue limited but significant activity in specific cellular contexts (Schuetz et al. 2008). It is also possible that Class IIa HDACS are specific for other, not yet identified post-translational modifications. Alternatively, they may act as binders of acetyl marks in the nucleus or cytoplasm where they shuttle once phosphorylated, a model supported by two observations: HDAC7 has an affinity comparable to other HDACs for acetylated peptides (Hildmann et al. 2006; Schuetz et al. 2008), and an acetylated lysine peptide potently inhibits Class IIa enzymatic activity against a more labile trifluoroacetylated substrate (Bradner et al.). Finally, Class IIa HDACs are part of multiprotein complexes, and may simply act as docking platforms for other proteins, such as transcription factors and more active HDACs, as suggested by the observation that they only regulate transcription

by recruiting SMRT/N-CoR□HDAC3, regardless of their enzymatic activity (Fischle et al. 2001; Fischle et al. 2002).

Inhibitor specificity

A pharmacophore model of HDAC inhibitors previously proposed is composed of a cap that sits at the rim of the substrate channel, a chelator that occupies the bottom of the channel and interacts with the Zn ion, and a linker that bridges the cap and the chelator (Miller et al. 2003). This model still holds, but, based on recent structures, should probably be complemented with a fourth optional element that we name the foot, and occupies the so-called foot-pocket present in some isoforms (Figure 7A). We will now review the structural chemistry of these different elements in the light of available complex structures of human HDACs (Figure 8).

The cap of HDAC inhibitors varies in its chemical nature and orientation from one isoform to another, and within single isoforms. For instance, TSA, APHA and N-hydroxy-4-{methyl[(5-pyridin-2-yl-2-thienyl)sulfonyl]amino}benzamide (referred to as PTSB-hydroxamate) all occupy different areas of the rim in HDAC8, formed by the flexible loops discussed above: TSA, mainly contacts loop L2, APHA loop L3 and PTSB-hydroxamate loop L1 (Figure 7B-D). It should be noted that the conformations observed may also be influenced by intermolecular contacts with crystallographic dimers. Not surprisingly, smaller capping elements, such as the phenyl ring of SAHA, make fewer interactions with the rim, are more flexible - as revealed by the absence of electronic density in the complex structure with HDAC7 ((Schuetz et al. 2008) [3c0z]) - and contribute less to binding, while the larger cap of a substrate-inspired HDAC8 inhibitor contributes significantly to binding enthalpy through its methoxy-indole ring and a pair of amide nitrogens engaged in multiple hydrogen bonds with the conserved Asp101 (figure not shown, (Vannini et al. 2007) [2v5x]). A potent cap-less HDAC2 inhibitor was recently crystallized entirely buried in the lysine channel, in a conformation that extends deeply into a foot pocket, showing that the capping moiety is an optional feature, as long as sufficient interactions are provided by other elements (Bressi et al.) (Figure 7E).

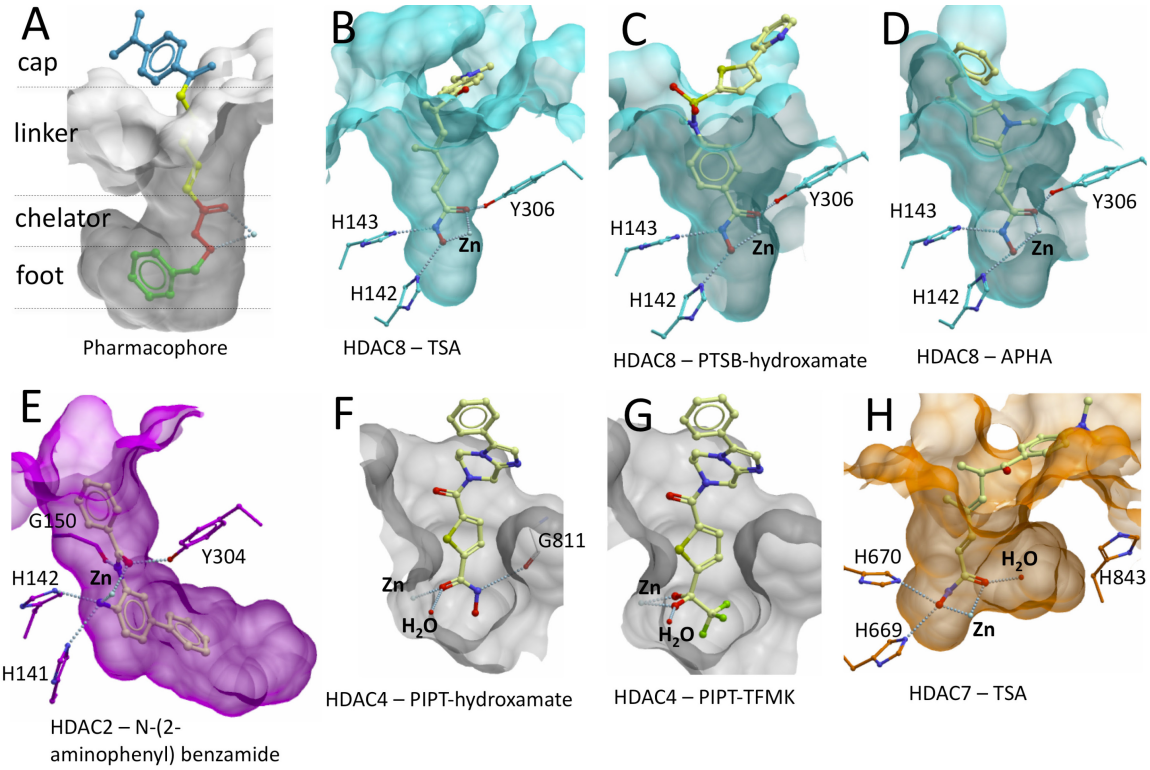

Figure 7: Structural chemistry of HDAC inhibitors. (A) Pharmacophoric scheme: HDAC inhibitors are composed of a capping end, a linker, and a zinc chelating moiety. An additional group can in some cases extend beyond the catalytic center, into a foot pocket. B-D: Compounds with diverse linkers were co-crystallized with HDAC8. B: TSA ([1t64], (Somoza et al. 2004)) C: PTSB-hydroxamate ([1w22], (Vannini et al. 2004)) D: APHA ([3f07], (Dowling et al. 2008)). E: HDAC2 was solved in complex with a cap-less inhibitor that features a non-hydroxamate chelating group and a foot that occupies a cavity at the entrance of the by-product exit channel ([3max], (Bressi et al.)). F,G: The HDAC4 channel can adopt a partly open conformation that could accommodate larger linkers. F: The protonated hydroxamic acid adopts an unfavorable monodentate chelation mode ([2vqm], (Bottomley et al. 2008)); G: the hydrated trifluoromethyl ketone is a better chelating agent ([2vqj], (Bottomley et al. 2008)). H: The HDAC7-TSA complex features a foot pocket that may be exploited to achieve selectivity ([3c10], (Schuetz et al. 2008)).

Varying uniquely the capping moiety in a library of para-substituted cinnamic hydroxamic acids resulted in IC50 values ranging from 20 nM to over 50 microM against HDAC5, which suggests that the capping feature can be a used as a driver of specificity (Bradner et al.). However, such strategy is probably unreliable, as it is resting on interactions with a very malleable surface composed of flexible loops. The latter may adopt alternate conformations to accommodate inhibitor binding, as observed in HDAC4, where the capping element of the inhibitor is suspected to

contribute to major conformational rearrangement of loops L1 and L2, which may alter functional protein interaction events (Figure 3C).

Ligand Name	Gene	PDB Code	Reference
APHA	HDAC8	3f07	1
CRA-19156	HDAC8	1vkg	2
IPIO-hydroxamate	HDAC8	2v5x	3
MS-344	HDAC8	1t67, 3mz3/4/6/7, 3ew8, 3f06, 3ezp/t	1,2,4
N-(2-aminophenyl) benzamide	HDAC2	3max	5
PIPT-hydroxamate	HDAC4	2vqm/v	6
PIPT-TFMK	HDAC4	2vqj/o/q	6
PTSB-hydroxamate	HDAC8	1w22	7
SAHA	HDAC7	3c0z	8
	HDAC8	1t69	2
TSA	HDAC7	3c10	8
	HDAC8	1t64, 3f0r	1,2

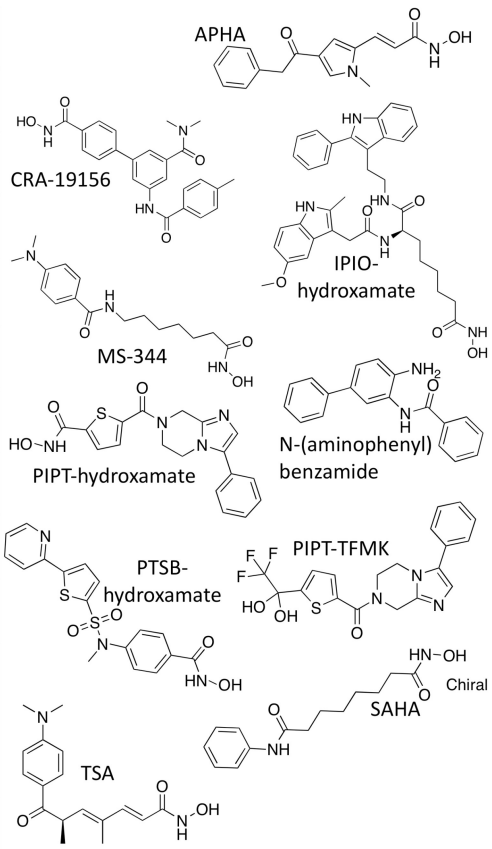

Figure 8: Publically available structures of human HDACs in complex with inhibitors. References: 1: (Dowling et al. 2008), 2: (Somoza et al. 2004), 3: (Vannini et al. 2007), 4: (Dowling et al.), 5: (Bressi et al.), 6: (Bottomley et al. 2008), 7: (Vannini et al. 2004), 8: (Schuetz et al. 2008)

The linker element needs to accommodate the geometry of the lysine channel, while maintaining an acceptable pose at the capping end and complying with the very strict structural constraints imposed by the orientation of the chelator, as detailed later. Structures of inhibitors with different linkers in complex with HDAC8 reveal how diverse scaffolds can occupy the same lysine channel, while keeping the orientation of the hydroxamate chelator absolutely unchanged (Figure 7B-D).

Linkers that better occupy the lysine channel while maintaining favorable orientations at the capping and chelating ends are expected to better contribute to binding. The width of the channel is not absolutely conserved between the different HDAC isoforms, which may open some opportunity to engineer specificity: a bulkier linker may still fit in the wider channel of HDAC7, but not that of HDAC2 (Figure 7 E,H). The large conformational rearrangement of HDAC4 loops induced by the cap of phenyl-imidazo-pyrazin-thiophenyl (PIPT) inhibitors results in a partial opening of the lysine channel (Figure 8 F,G). This surprising mechanism seems particularly fitted to design HDAC4-selective compounds. The observation that HDAC7 is more susceptible to cinnamic hydroxamic acids harboring a para- versus meta-substituted linker, while no distinction is observed for HDAC2, HDAC3 and HDAC7, confirms that, at least in some cases, linker chemistry can be exploited to achieve selectivity (Bradner et al.).

The canonical chelating group of HDAC inhibitors is hydroxamic acid. The mechanism of binding has conserved features with zinc metalloprotease hydroxamate inhibitors (Grams et al. 1995). Typically, both carbonyl and hydroxyl oxygen atoms participate in zinc coordination in a bidentate manner (Figure 7B-D). Two conserved catalytic histidines are engaged in hydrogen-bonds with the oxygen and nitrogen of the hydroxylamine. Another hydrogen bond is formed between the carbonyl oxygen and the catalytic tyrosine. It is speculated that this network of hydrogen-bonds would lower the pKa and facilitate deprotonation of the chelator, which would result in tighter binding (Bradner et al. ; Wang et al. 2007). This argument is supported by the observation that hydroxamic acid-based inhibitors are less potent against Class IIa HDACs, where the catalytic tyrosine is absent (Bradner et al.). Structures of HDAC4 and HDAC7 in complex with hydroxamic inhibitors reveal that a water molecule is hydrogen-bonded to the chelating carbonyl in place of the catalytic tyrosine, while interactions with the histidine are lost in HDAC4, and exclusively directed at the hydroxyl oxygen in HDAC7 (Figure 7-F,H). Consequently, a monodentate chelating mode is observed in HDAC4, while a sub-optimal bidentate geometry may take place in the HDAC7 complex where the

distinction between mono and bidentate orientation is probably not within resolution limits. The altered network of interaction, geometry, and suspected protonation state in class IIa HDACs is in agreement with the observation that hydroxamic acids are ten to hundred folds more potent against gain-of function HDAC4 or HDAC7 mutants where the catalytic tyrosine has been restored (Bottomley et al. 2008; Schuetz et al. 2008).

The mode of binding of non-hydroxamate chelators has recently been elucidated in complex with class I and class IIa enzymes. The crystal structure of HDAC2 bound to a potent o-amino-anilide based inhibitor revealed that the amine nitrogen and amide carbonyl could recapitulate bidentate chelation of the zinc ion as well as hydrogen bonding with the catalytic histidine and tyrosine residues. The amide nitrogen is making an additional bond with the carbonyl oxygen of G150 (Figure 7E). A hydrated trifluoromethyl ketone bound to HDAC4 is also chelating the catalytic zinc in a bidentate geometry via its two oxygen atoms (Figure 7F). Interestingly the same compound with a hydroxamic acid chelating group is about three times less potent, but has an activity increased 30 fold against the H976Y gain-of function mutant, while the activity of the trifluoromethyl ketone remains unchanged at about 300 nM IC50 (Bottomley et al. 2008). This, along with recent observations that hydroxamic acid compounds are suboptimal against class IIa HDACs (Bradner et al.), suggests that hydrated trifluoromethyl ketones may be better suited towards this class of enzymes.

The recent structure of HDAC2 in complex with an o-amino-anilide inhibitor revealed a large foot pocket occupied by a diphenyl moiety (Bressi et al.) (Figure 7E). The pocket is located at the entrance of the narrow exit channel for the acetate by-product discussed above. The cavity is occupied by a proline residue in class IIa structures (P667 in HDAC7), due to different protein backbone conformation. The protein backbone is conserved between HDAC2 and HDAC8, but in the latter, the side-chain of Trp 141 partially obstructs the foot pocket. The corresponding residue is a leucine in HDAC1,2 and 3 (Figure 1), suggesting that this foot pocket is

conserved in some isoforms. The selectivity profile of compounds occupying this cavity remains to be documented.

The crystal structure of HDAC7 in complex with inhibitors also revealed the presence of a foot pocket with a geometry distinct from that observed in HDAC2 (Schuetz et al. 2008) (Figure 7H). This time, the pocket is generated by the conformation of the class IIa specific His 843 that is flipped away from the active site. In class I enzymes, this cavity is occupied by the catalytic tyrosine, that forms a hydrogen bond with the substrate or the chelating group of inhibitors. This pocket is expected to be conserved in class IIa enzymes, even though it was not observed in available wild type HDAC4 structures due to the large opening of the lysine channel induced by the co-crystallized inhibitors.

Limited protein availability and lack of adequate substrates have seriously challenged efforts to systematically characterize and rationalize the selectivity profile of HDAC inhibitors. Recent progress in assay development (Bradner et al.), and novel structural data are now crystallizing into a formalized understanding of HDAC inhibition, which should accelerate the development of compounds with diverse selectivity profiles, help dissect the cellular biology of protein deacetylation, and contribute to the discovery of better targeted clinical candidates.

Conclusion

The structural mechanism of class I and class IIa HDACs is now well understood, and relies on interconnected elements involved in substrate recognition and catalysis. The chemistry of competitive inhibitors articulates around a well-established conceptual framework derived from available complex structures. This understanding will allow the development of class- and isoform-specific compounds with novel chemotypes and should result in a chemogenomic coverage of metal-dependent HDACs with clinical impact.

The biological reality that HDACs generally operate within large protein complexes remains however structurally unexplored. What are the conformational

rearrangements induced by diverse functional binding partners, and what are there consequences on enzymatic activity? What are the contributions of structural elements outside of the catalytic domain to substrate recognition and HDAC biology? Are class IIa HDACs activated within specific multiprotein complexes? Or are they, as bromodomains, simply readers of acetyl marks, or sensors of other post-translational modifications? Are novel allosteric sites present within multisubunit complexes, and are these druggable? The structural biology of metal-dependent HDACs remains in many ways a mystery.

Acknowledgements:

This work was supported by the Structural Genomics Consortium. The SGC is a registered charity (number 1097737) that receives funds from the Canadian Institutes for Health Research, the Canadian Foundation for Innovation, Genome Canada through the Ontario Genomics Institute, GlaxoSmithKline, Karolinska Institutet, the Knut and Alice Wallenberg Foundation, the Ontario Innovation Trust, the Ontario Ministry for Research and Innovation, Merck & Co., Inc., the Novartis Research Foundation, the Swedish Agency for Innovation Systems, the Swedish Foundation for Strategic Research and the Wellcome Trust.

References:

Ago T, Liu T, Zhai P, Chen W, Li H, Molkentin JD, Vatner SF, Sadoshima J (2008) A redox-dependent pathway for regulating class II HDACs and cardiac hypertrophy. Cell 133: 978-93

Bottomley MJ, Lo Surdo P, Di Giovine P, Cirillo A, Scarpelli R, Ferrigno F, Jones P, Neddermann P, De Francesco R, Steinkuhler C, Gallinari P, Carfi A (2008) Structural and functional analysis of the human HDAC4 catalytic domain reveals a regulatory structural zinc-binding domain. J Biol Chem 283: 26694-704

Bradner JE, West N, Grachan ML, Greenberg EF, Haggarty SJ, Warnow T, Mazitschek R Chemical phylogenetics of histone deacetylases. Nat Chem Biol 6: 238-243

Bressi JC, Jennings AJ, Skene R, Wu Y, Melkus R, De Jong R, O'Connell S, Grimshaw CE, Navre M, Gangloff AR Exploration of the HDAC2 foot pocket: Synthesis and SAR of substituted N-(2-aminophenyl)benzamides. Bioorg Med Chem Lett 20: 3142-5

Choudhary C, Kumar C, Gnad F, Nielsen ML, Rehman M, Walther TC, Olsen JV, Mann M (2009) Lysine acetylation targets protein complexes and co-regulates major cellular functions. Science 325: 834-40

Dowling DP, Gantt SL, Gattis SG, Fierke CA, Christianson DW (2008) Structural studies of human histone deacetylase 8 and its site-specific variants complexed with substrate and inhibitors. Biochemistry 47: 13554-63

Dowling DP, Gattis SG, Fierke CA, Christianson DW Structures of metal-substituted human histone deacetylase 8 provide mechanistic inferences on biological function. Biochemistry 49: 5048-56

Finnin MS, Donigian JR, Cohen A, Richon VM, Rifkind RA, Marks PA, Breslow R, Pavletich NP (1999) Structures of a histone deacetylase homologue bound to the TSA and SAHA inhibitors. Nature 401: 188-93

Fischle W, Dequiedt F, Fillion M, Hendzel MJ, Voelter W, Verdin E (2001) Human HDAC7 histone deacetylase activity is associated with HDAC3 in vivo. J Biol Chem 276: 35826-35

Fischle W, Dequiedt F, Hendzel MJ, Guenther MG, Lazar MA, Voelter W, Verdin E (2002) Enzymatic activity associated with class II HDACs is dependent on a multiprotein complex containing HDAC3 and SMRT/N-CoR. Mol Cell 9: 45-57

Gantt SL, Gattis SG, Fierke CA (2006) Catalytic activity and inhibition of human histone deacetylase 8 is dependent on the identity of the active site metal ion. Biochemistry 45: 6170-8

Grams F, Crimmin M, Hinnes L, Huxley P, Pieper M, Tschesche H, Bode W (1995) Structure determination and analysis of human neutrophil collagenase complexed with a hydroxamate inhibitor. Biochemistry 34: 14012-20

Gregoretti IV, Lee YM, Goodson HV (2004) Molecular evolution of the histone deacetylase family: functional implications of phylogenetic analysis. J Mol Biol 338: 17-31

Grozinger CM, Schreiber SL (2002) Deacetylase enzymes: biological functions and the use of small-molecule inhibitors. Chem Biol 9: 3-16

Hildmann C, Wegener D, Riester D, Hempel R, Schober A, Merana J, Giurato L, Guccione S, Nielsen TK, Ficner R, Schwienhorst A (2006) Substrate and inhibitor specificity of class 1 and class 2 histone deacetylases. J Biotechnol 124: 258-70

Kanyo ZF, Scolnick LR, Ash DE, Christianson DW (1996) Structure of a unique binuclear manganese cluster in arginase. Nature 383: 554-7

Lahm A, Paolini C, Pallaoro M, Nardi MC, Jones P, Neddermann P, Sambucini S, Bottomley MJ, Lo Surdo P, Carfi A, Koch U, De Francesco R, Steinkuhler C, Gallinari P (2007) Unraveling the hidden catalytic activity of vertebrate class IIa histone deacetylases. Proc Natl Acad Sci U S A 104: 17335-40

Lee H, Rezai-Zadeh N, Seto E (2004) Negative regulation of histone deacetylase 8 activity by cyclic AMP-dependent protein kinase A. Mol Cell Biol 24: 765-73

Marks PA The clinical development of histone deacetylase inhibitors as targeted anticancer drugs. Expert Opin Investig Drugs 19: 1049-66

Miller TA, Witter DJ, Belvedere S (2003) Histone deacetylase inhibitors. J Med Chem 46: 5097-116

Nicolas E, Yamada T, Cam HP, Fitzgerald PC, Kobayashi R, Grewal SI (2007) Distinct roles of HDAC complexes in promoter silencing, antisense suppression and DNA damage protection. Nat Struct Mol Biol 14: 372-80

Nielsen TK, Hildmann C, Dickmanns A, Schwienhorst A, Ficner R (2005) Crystal structure of a bacterial class 2 histone deacetylase homologue. J Mol Biol 354: 107-20

Sauve AA, Wolberger C, Schramm VL, Boeke JD (2006) The biochemistry of sirtuins. Annu Rev Biochem 75: 435-65

Schuetz A, Min J, Allali-Hassani A, Schapira M, Shuen M, Loppnau P, Mazitschek R, Kwiatkowski NP, Lewis TA, Maglathin RL, McLean TH, Bochkarev A,

Plotnikov AN, Vedadi M, Arrowsmith CH (2008) Human HDAC7 harbors a class IIa histone deacetylase-specific zinc binding motif and cryptic deacetylase activity. J Biol Chem 283: 11355-63

Somoza JR, Skene RJ, Katz BA, Mol C, Ho JD, Jennings AJ, Luong C, Arvai A, Buggy JJ, Chi E, Tang J, Sang BC, Verner E, Wynands R, Leahy EM, Dougan DR, Snell G, Navre M, Knuth MW, Swanson RV, McRee DE, Tari LW (2004) Structural snapshots of human HDAC8 provide insights into the class I histone deacetylases. Structure 12: 1325-34

Vannini A, Volpari C, Filocamo G, Casavola EC, Brunetti M, Renzoni D, Chakravarty P, Paolini C, De Francesco R, Gallinari P, Steinkuhler C, Di Marco S (2004) Crystal structure of a eukaryotic zinc-dependent histone deacetylase, human HDAC8, complexed with a hydroxamic acid inhibitor. Proc Natl Acad Sci U S A 101: 15064-9

Vannini A, Volpari C, Gallinari P, Jones P, Mattu M, Carfi A, De Francesco R, Steinkuhler C, Di Marco S (2007) Substrate binding to histone deacetylases as shown by the crystal structure of the HDAC8-substrate complex. EMBO Rep 8: 879-84

Verdin E, Dequiedt F, Kasler HG (2003) Class II histone deacetylases: versatile regulators. Trends Genet 19: 286-93

Wang D, Helquist P, Wiest O (2007) Zinc binding in HDAC inhibitors: a DFT study. J Org Chem 72: 5446-9

Xu WS, Parmigiani RB, Marks PA (2007) Histone deacetylase inhibitors: molecular mechanisms of action. Oncogene 26: 5541-52

Yang XJ, Seto E (2003) Collaborative spirit of histone deacetylases in regulating chromatin structure and gene expression. Curr Opin Genet Dev 13: 143-53